

## PERFORMANCE COMPARISON OF ABOVEGROUND AND UNDERGROUND SOLAR PONDS

by

**Haci SOGUKPINAR<sup>a</sup>, Ismail BOZKURT<sup>b\*</sup>, and Mehmet KARAKILCIK<sup>c</sup>**

<sup>a</sup> Department of Electric and Energy, Vocational School, University of Adiyaman, Adiyaman, Turkey

<sup>b</sup> Department of Mechanical Engineering, Faculty of Engineering, University of Adiyaman, Adiyaman, Turkey

<sup>c</sup> Department of Physics, Faculty of Sciences and Letters, University of Cukurova, Adana, Turkey

Original scientific paper

<https://doi.org/10.2298/TSCI160613269S>

*This paper deals with the modeling of two different solar ponds which has some different structural parameters such as aboveground and underground, and its performance evaluation. The solar pond system generally consists of three zones, and the densities of these zones decrease from the bottom of the pond to the surface. The most significant decrease in the density distribution of the salt between bottom and up of the pond is the gradient zone. The convective heat loss in the solar pond is prevented with this zone. In this study, aboveground and underground solar ponds were modeled at the same dimensions, but different structural parameters in the same conditions. In this model, the temperature distributions of the solar pond were obtained during a year. The thermal performances of the solar pond were calculated and the results were compared with an experiment. This study shows that the efficiency of the aboveground solar pond is observed to be a maximum of 25.93% in July, a minimum of 4.53% in January. Furthermore, the efficiency of the underground solar pond is observed to be a maximum of 21.49% in July, a minimum of 6.55% in January. This study indicates that the underground construction of solar ponds, designed to be insulated using appropriate insulation materials, is found to be more efficient with respect to the aboveground pond.*

Key words: solar energy, solar pond, performance analysis

### Introduction

Many types of renewable energy resources such as solar, wind, geothermal, hydroelectric, and biomass, etc. can be used instead of fossil fuels. Because of the desirable environmental and safety aspects, it is widely believed that solar energy should be utilized instead of other renewable energy forms because it can be provided sustainably without harming the environment [1]. A solar pond is an important solar energy system with a simple structure and long-term heat storage features. The solar pond was discovered as a natural phenomenon around the turn of the last century in the Medve Lake in region of Transylvania, Hungary. In this lake, temperatures up to 70 °C were recorded at a depth of 1.32 m at the end of the summer season [2].

\* Corresponding author, e-mail: [ibozkurt@adiyaman.edu.tr](mailto:ibozkurt@adiyaman.edu.tr)

A solar pond consists of the layers which are increasing density toward the bottom. The convective heat loss in the solar pond is prevented with this construction. Thus, it is possible to store heat for a long time in the solar pond. The use of solar ponds is very important in many applications that need a large quantity of hot water, such as heating buildings, production electricity, desalination of sea water, textile processing, and food industries [3]. In this regard, many studies on model solar ponds have been done similar to the natural solar pond. Karakilcik *et al.* [4-8] studied thermal performance of the aboveground solar ponds. In these studies, experimental and theoretical temperature distributions, energy and exergy efficiencies, energy efficiencies for with and without shading area, and energy and exergy efficiencies of the integrated system were investigated. Also, aboveground solar ponds were studied by Bozkurt *et al.* [9-15]. In the studies, energy efficiencies depend on the number of collectors, effect of the transparent covers, comparison of the temperature distribution between conventional and integrated solar pond, effect of the sunny area ratios on thermal efficiency of model solar pond for different cases, energetic and exergetic performance of a solar pond integrated with four flat plate solar collectors, performance evaluation of a magnesium chloride saturated solar pond were investigated. Bezir *et al.* [16] investigated the numerical modeling developed for a salt gradient solar pond having covers used for preventing heat loss and reflecting the sunlight into the solar pond. Generally, solar ponds with large surface areas are built underground. Nie *et al.* [17] built a solar pond which has an area of 2500 m<sup>2</sup> and is 1.9 m deep. The solar pond started operation in spring when the ambient temperature was very low and has operated steadily for 105 days, with local climate zone (LCZ) temperature varying between 20 and 40 °C. Kayali *et al.* [18] investigated a mathematical model of a rectangular solar pond. The 1- and 2-D heat balance equations were written, in finite difference form, on the brine and the soil surrounding the pond. In addition, using meteorological data for the Cukurova region of Turkey, empirical functions for ambient air and soil temperatures were developed. Kumar and Kishore [19] constructed a 6000 m<sup>2</sup> solar pond at city of Bhuj, India, in the premises of a milk processing dairy plant to supply heat process and demonstrate the technical and economic viability of solar pond technology in the Indian context. Saleh *et al.* [20] investigated a solar pond near the Dead Sea, Middle East, and coupled with a flash desalination plant. It was found that a 3000 m<sup>2</sup> solar pond installed near the Dead Sea is able to provide an annual average production rate of 4.3 L/min distilled water. Bernad *et al.* [21] developed a numerical model based on the overall energy balance of the pond to predict energy performance of a preindustrial scale solar pond by considering the heat storage efficiency. Akbarzadeh *et al.* [22] investigated the use of a chimney with a turbine as a potentially simple alternative to ORC engines and as a compatible energy converter for integration with solar ponds. Ranjan *et al.* [23] studied energy and exergy analyses of a salinity-gradient solar pond (100 × 100 m) for Indian climatic conditions. It was found that the highest amount of useful low-grade thermal energy, *i. e.*, 24260 and 28119 MJ, can be extracted at 80 and 85 °C temperatures from heat storage zone (HSZ).

Many studies have been done about solar ponds with different sizes and features [4-23]. For all that, there have not been any investigations on energy efficiency comparison of the aboveground and underground solar ponds at the same dimensions and conditions. This was, in fact, the key motivation behind the present work. In this work, aboveground and underground solar ponds were simulated. The temperature distributions of the solar pond were determined during a year at the same dimensions and conditions. Furthermore, the thermal performances of the solar pond were calculated.

### Modeling of solar pond and Its structure

Solar ponds that collect solar energy are capable of storing heat energy for a long time. The artificial solar ponds can be constructed similarly to the natural solar pond. As shown in fig. 1, solar ponds usually consist of three regions. High-density region in the bottom of the pond is called HSZ. The region consists of layers, where density decreases from HSZ to the surface of the pond, is called non-convective zone (NCZ). Salt water can not rise in NCZ because the brine layer on that has less density. Likewise, it could not get down because there is more density salt water just below. This prevents heat loss by convection at HSZ. The HSZ heat losses only happen by conduction. The NCZ acts as a transparent insulator which allows the sunlight to pass HSZ and also prevents heat loss by convection. The region on NCZ consists of fresh water is called upper convective zone (UCZ). Heat energy is collected and stored in HSZ. In this study, two solar ponds  $2 \times 2 \times 1.5$  m in size were compared. One of them is aboveground, and the other is constructed underground. These solar ponds were modeled at the same conditions. Physical characteristics of the solar ponds are given in fig. 1.

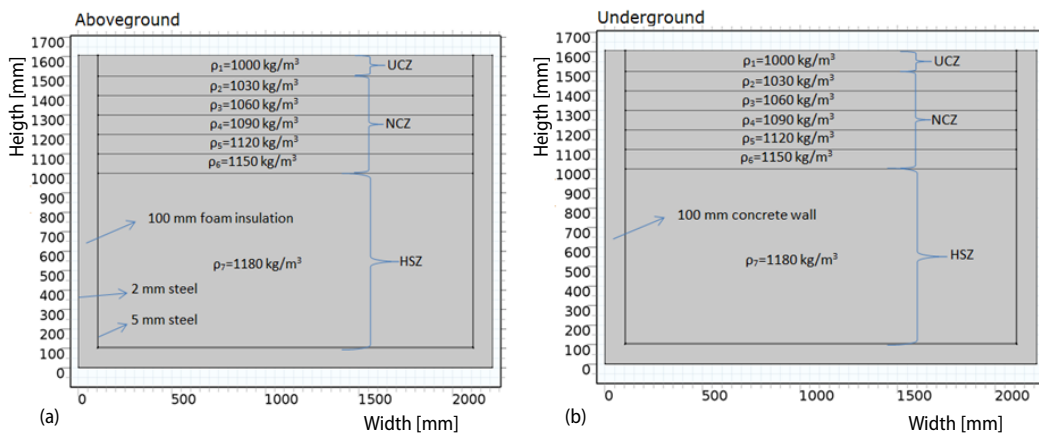


**Figure 1. Computational domain for aboveground and underground conditions and boundary requirement**

The first law of thermodynamics applies to all heat transfer which is the principle of conservation of energy. Basic heat transfer equation is written in terms of temperature [24]:

$$\rho C_p \left[ \frac{\partial T}{\partial t} + (u \nabla) T \right] = -\nabla (q_c + q_r) + \tau : \mathbf{S} - \frac{T}{\rho} \frac{\partial \rho}{\partial T} \left[ \frac{\partial p}{\partial t} + (u \nabla) p \right] + Q \quad (1)$$

Numbers of thermodynamic equations are used to derive eq. (1) and for the equation, it is also assumed that mass is always conserved. The relationship between speed and density is expressed:

$$\frac{\partial \rho}{\partial t} + \nabla (\rho v) = 0 \quad (2)$$

Radiation in participating media heat transfer equation in any direction ( $\Omega$ ) is expressed with [25]:

$$\Omega \nabla I(\Omega) = \kappa I_b(T) - \beta I(\Omega) + \frac{\sigma_s}{4\pi} \int_0^4 I(\Omega') \phi(\Omega', \Omega) d\Omega' \quad (3)$$

where  $I(\Omega)$  is radiation intensity,  $\kappa, \beta, \sigma_s$  are absorption, extinction, and scattering coefficient, respectively. The  $\Omega_{i+}$  is given (4) [26]:

$$\Omega_{i+} \nabla I_{i+} = \kappa I_b(T) - \beta I_{i+} + \frac{\sigma_s}{4\pi} \sum_{j=1}^n \omega_j I_j \Phi(\Omega_j, \Omega_{i+}) \quad (4)$$

The COMSOL software was used to solve these equations. When solving the equation there is only one standard model input which is temperature [K] and the default absorption coefficient,  $\kappa$  [ $\text{m}^{-1}$ ], uses the value from material but values can be changed. The default scattering coefficient,  $\sigma_s$  [ $\text{m}^{-1}$ ], also uses the value from material but user defined can be selected. For the scattering type there are three option they are isotropic, linear anisotropic, and polynomial anisotropic. The opaque surface nodule defines a boundary opaque region to radiation. For the wall setting there are two option and they are gray wall and black wall. Computational domains for the aboveground and underground condition are shown in fig. 1. Aboveground and underground domain consists of seven layers. In the first 6 layers from top to bottom, layer height is 0.10 m and the last layer is 0.90 m in height. An exterior wall of aboveground pond is surrounded by 0.002 m and interior wall is surrounded by 0.005 m thick steel plate and there are 0.10 m insulation materials in between these two plates. All boundary surfaces for above ground pond are contacted with air. For underground pond, there is only 0.10 m thick concrete wall in the soil.

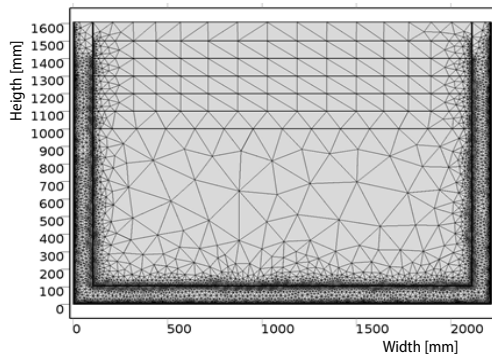


**Figure 2. Mesh distributions of the model solar pond**

**Table 1. Computational conditions**

Wall types	Gray
Present study	Time dependent
Initial temperature	305.78 K
Reference temperature	293.15 K
Reference pressure	1 atm
Method	Discrete ordinate methods
Discretization level	linear
Wall height	1600

ing the surface of the pond. To determine the stored heat by aboveground and underground solar pond, the temperature distributions in the solar pond were calculated. At aboveground solar pond, heat loss from the entire surface of the walls is carried out with convection but in

For the meshing, COMSOL software is used to generate the computational grid and for this calculation physics controlled meshing types and extremely coarse element sizes are chosen. Because no needs to use too dense grid numbers for this calculation. Sometimes too dense or too sparse grid may produce calculation results with a large error. Therefore, the effect of the grid number on the numerical solution is carefully tested in the preliminary calculation. Discretized domain is optimized based on the number of cells and the cell shape and the final mesh used in the simulation is shown in fig. 2. Also, computational conditions are given in tab. 1 for this model.

### Energy analysis of solar pond

It is very important to determine the performance of the solar pond. The performance of solar pond depends on the differences of inner and outer parameters (*e. g.*, pond dimensions, insulation materials, shading effect). For the model, we consider the following key parameters: air and soil temperature, initial temperature distribution, and incident radiation reach-

the walls and inside the pond it happens with by conduction. For underground solar pond, it is unlike aboveground because side wall of the pond is under the ground and in contact with the soil so heat loss except for upper side of the pond is carried out with conduction. The radiation heat loss of the solar pond was neglected because solar ponds' temperature is low. Furthermore, the convection heat loss from the solar pond is prevented by NCZ so these heat losses were not considered in the model. Thus, the energy efficiency of solar pond can be defined as [14]:

$$\eta = \frac{E_{\text{stored}}}{E_{\text{in}}} = 1 - \frac{E_{\text{bottom}} + E_{\text{up}} + E_{\text{side}}}{E_{\text{in}}} \quad (5)$$

where  $E_{\text{stored}}$  is stored heat energy in HSZ of the solar pond,  $E_{\text{in}}$  – the amount of net solar energy absorbed by HSZ,  $E_{\text{bottom}}$  – the total heat loss to the bottom wall,  $E_{\text{up}}$  – the heat loss from HSZ to the above zone, and  $E_{\text{side}}$  – the total heat loss to the side walls. Substituting equations for each parameter in eq. (1) provides us with the following energy efficiency of solar pond [14]:

$$\eta = 1 - \frac{\left[ \frac{k_w A}{\Delta x_{\text{bottom}}} (T_{\text{bottom}} - T_{\text{sur.}}) + \frac{k_s A}{\Delta x_{\text{HSZ-NCZ}}} (T_{\text{HSZ}} - T_{\text{NCZ}}) + \frac{k_w A_{\text{side}}}{\Delta x_{\text{side}}} (T_{\text{HSZ}} - T_{\text{sur.}}) \right]}{\beta EA [(1-F) h(x_l - \delta)]} \quad (6)$$

where  $\beta$  is the fraction of the incident solar radiation and it is given by Duffie and Beckman [27]:

$$\beta = 1 - 0.5 \left[ \frac{\sin^2(\theta_i - \theta_r)}{\sin^2(\theta_i + \theta_r)} + \frac{\tan^2(\theta_i - \theta_r)}{\tan^2(\theta_i + \theta_r)} \right] \quad (7)$$

Here  $h$  represents the ratio of the solar energy reaching the depth  $X$  is given by Bryant and Colbeck [28]:

$$h = 0.36 - 0.08 \ln \left( \frac{X}{\cos \theta_r} \right) \quad (8)$$

where  $X$  is the depth of water in meter. The COMSOL software was used to determine the temperature distribution and heat loss.

## Results and discussion

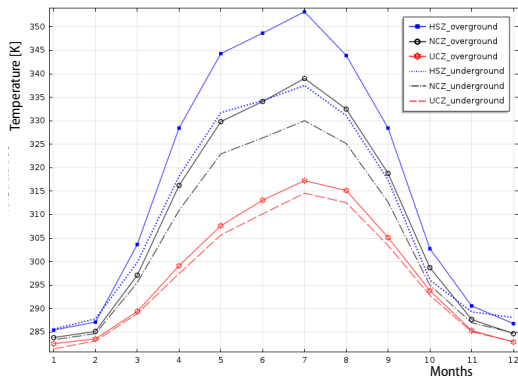
In this study, the temperature distributions were calculated. Furthermore, the energy efficiencies of the model solar ponds were calculated by using the temperature distribution. In the model, the key parameters such as air and soil temperature, and incident radiation were used. The temperature variation in the soil for the underground pond is very important. Soil temperature is higher than the air temperature in the winter, while in summer it is at lower levels. However, soil temperature variation within the year is less than the range of variation of the air temperature. Table 1 listed air and soil (for 0.10 m depth) temperature and solar radiation intensities. When tab. 2 is examined, it is realized that average maximum temperature of 32.63 °C is observed in August and a minimum of 7.62 °C in January. Soil temperature is realized with maximum 26.6 °C in August and a minimum of 13.3 °C in January. It is understood that the difference between the maximum and minimum temperatures for air is 25.01 °C and for soil, it is 13.30 °C. The change in soil temperature during the year with the change of air temperature is seen to be quite low. However, it is measured that the average the maximum solar energy intensity on a flat surface is 287.62 W/m<sup>2</sup> in July and minimum with the value 65.47 W/m<sup>2</sup> in January.

**Table 2. The parameters of air and soil (for 0.10 m depth) temperature and solar radiation intensities**

Month	Air temperature [°C]	Soil temperature [°C]	Solar radiation [ $Wm^{-2}$ ]
Jan.	7.62	13.30	65.47
Feb.	9.45	14.70	84.35
Mar.	12.26	16.40	154.08
Apr.	17.15	19.60	219.09
May	22.14	22.80	265.89
June	26.78	24.20	275.28
July	31.94	25.30	287.62
Aug.	32.63	26.60	258.80
Sept.	25.45	24.10	208.20
Oct.	18.53	21.80	140.46
Nov.	11.07	18.30	118.24
Dec.	9.08	14.20	73.67

Temperature distribution in the solar pond is affected by ambient temperature, rainfall, and solar energy and used insulation materials. The UCZ forms the top layer of the solar pond and affected by the external conditions because it is in contact with the air. Heat lost from UCZ occurs with conduction from the side walls and with convection over the top surface. Temperature change in underground solar pond shows similar properties with aboveground pond. The air temperature is lower than soil in the winter months due to high soil temperature so the tempera-

ture of the underground solar pond is higher. Similarly, during the summer months due to the low temperature of the soil, the temperature of the over ground solar pond is greater.

**Figure 3. The temperature distributions of the zones for aboveground and underground solar pond during a year**

Solar pond temperature distribution increases toward the bottom of the pond similar to the density gradient. Aboveground and underground solar pond temperature distribution for HSZ, NCZ, and UCZ regions are shown in fig. 3, NCZ prevents heat loss with convection by acting as a transparent insulator in the pond. Thus, the storage zone temperature of the pond reaches a higher value than the upper zone. As shown in fig. 3, it is seen that maximum temperature in HSZ in July with the value of 350 K and 340 K for aboveground and underground, respectively. Likewise, it is seen that maximum temperature for July at NCZ with the value of 340 K and 330 K for aboveground and underground, respectively. The UCZ from

the surface of the pond and in contact with air. Therefore, the surface where the heat loss happens greatly affects the temperature of this region. The maximum temperature in July is observed in UCZ for aboveground and underground as 317 K and 315 K, respectively. It is understood that underground solar pond temperature in the winter is higher than aboveground pond.

The total heat loss from aboveground and underground solar ponds were calculated by using software program. Figure 4 shows the total heat loss for two different solar ponds during the year. As shown in fig. 4, the total heat loss from the aboveground solar pond is observed to be a maximum of 3534.25 MJ in June, a minimum of 1036.88 MJ in January. Furthermore, the total heat loss from the underground solar pond is observed to be a maximum of 3745.93 MJ in June, a minimum of 1014.92 MJ in January. The difference between the pond temperature and the ambient temperature are greater in the summer while in winter there is little difference. Therefore, heat losses in the summer is more than winter.

The efficiency of solar pond depends on inner and outer parameters (*e. g.*, pond dimensions, insulation materials, shading effect). Figure 5 shows the efficiency of the aboveground and underground solar ponds during a year. As shown in fig. 5, the efficiency of the aboveground solar pond is observed to be a maximum of 25.93% in July, a minimum of 4.53% in January. Furthermore, the efficiency of the underground solar pond is observed to be a maximum of 21.49% in July, a minimum of 6.55% in January. Here it is understood that by depending on the soil temperature, efficiency of the underground pond seems to be higher than the aboveground pond in winter months.

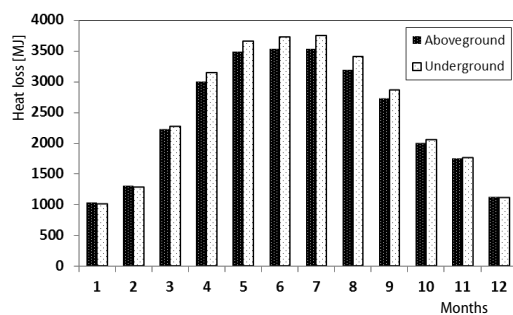


Figure 4. Total heat losses for aboveground and underground solar ponds

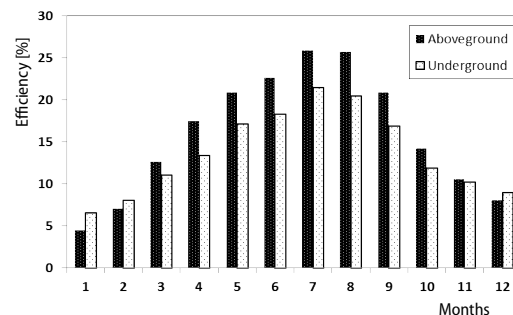


Figure 5. The heat storage efficiencies for aboveground and underground solar ponds

Table 3 shows the comparisons of both model and experimental results. The experimental study for aboveground solar pond was carried out by Karakilcik *et al.* [5]. The comparison made ponds have the same size and similar insulating properties. As seen in the table, the experimental and model distributions follow the same trend.

### Conclusion

In this study, we carried out numerical calculation for the temperature distribution of the aboveground and underground solar ponds to determine energy efficiency. For this purpose, a software program (COMSOL) was used. The temperature distributions of the solar pond depend on air temperature, heat losses and reached solar energy. A heat loss of the pond was calculated for one year by using air and soil temperature and solar radiation data from meteorology. In determining the performance of the pond, incident solar energy and heat losses from pond are taken into account. As a result, the underground construction of solar ponds, designed to be insulated using appropriate insulation materials, is found to be more efficient with respect to the aboveground pond.

### Acknowledgment

I thank Middle East Technical University, allowing me to this work in there with their facility.

Table 3. The comparison of the experimental and model energy efficiency

Month	Experimental [5]	Model
Jan.	9.68	4.53
Feb.	9.96	7.11
Mar.	10.9	12.69
Apr.	12.65	17.51
May	17.54	20.92
June	–	22.65
July	23.88	25.93
Aug.	28.11	25.73
Sept.	26.47	20.92
Oct.	25.67	14.23
Nov.	17.68	10.6
Dec.	13.28	8.11

## Nomenclature

$A$	– area, [m <sup>2</sup> ]
$C_p$	– heat capacity, [Jkg <sup>-1</sup> °C <sup>-1</sup> ]
$E$	– energy, [MJ]
$F$	– absorbed energy percentage at a region of $\delta$ -thickness, [%]
$h$	– heat transfer coefficient, [Wm <sup>-2</sup> K <sup>-1</sup> ].
$k$	– thermal conductivity, [Wm <sup>-1</sup> K <sup>-1</sup> ]
$n$	– number of day,
$p$	– pressure, [Pa]
$Q$	– heat sources other than viscous heating, [Wm <sup>-3</sup> ]
$q$	– heat flux by conduction, [Wm <sup>-2</sup> ]
$q_c$	– heat transfer by convection, [Wm <sup>-2</sup> K <sup>-1</sup> ]
$q_r$	– heat transfer by radiation, [Wm <sup>-2</sup> K <sup>-1</sup> ]
$\mathbf{S}$	– strain-rate tensor, [s <sup>-1</sup> ]
$T$	– temperature, [°C]
$t$	– time
$\mathbf{u}$	– velocity vector, [ms <sup>-1</sup> ]
$v$	– velocity, [ms <sup>-1</sup> ]
$\Delta x$	– thickness of horizontal layers, [m]

### Greek symbols

$\beta$	– incident beam entering rate into the water, [-]
---------	---

$\delta$	– thickness where the long wave solar radiation is absorbed, [m]
$\eta$	– thermal energy efficiency, [-]
$\theta$	– angle, [rad]
$\rho$	– density, [kgm <sup>-3</sup> ]
$\boldsymbol{\tau}$	– viscous stress tensor, [Pa]
$\phi$	– latitude angle, [rad]

### Subscripts

i	– incident
r	– refracted
s	– salty water
side	– side wall
stored	– stored heat
sur.	– surrounding
up	– just above zone
w	– wall

### Acronyms

HSZ	– heat storage zone
NCZ	– non-convective zone
UCZ	– upper convective zone

## References

- [1] Kalogirou, S. A., *Solar Energy Engineering Processes and Systems*, 1<sup>st</sup> ed., Cyprus University of Technology, Limansol, Cyprus
- [2] El-Sebaï, A. A., *et al.*, History of the Solar Ponds: A Review Study, *Renewable and Sustainable Energy Reviews*, 15 (2011), 6, pp. 3319-3325
- [3] Boudhiaf, R., Baccar, M., Transient Hydrodynamic, Heat and Mass Transfer in a Salinity Gradient Solar Pond: A Numerical Study, *Energy Conversion and Management*, 79 (2014), Mar., pp. 568-580
- [4] Karakilcik, M., *et al.*, Experimental and Theoretical Temperature Distributions in a Solar Pond, *International Journal of Heat and Mass Transfer*, 49 (2006), 5-6, pp. 825-835
- [5] Karakilcik, M., *et al.*, Performance Investigation of a Solar Pond, *Applied Thermal Engineering*, 26 (2006), 7, pp. 727-735
- [6] Karakilcik, M., Dincer, I., Exergetic Performance Analysis of a Solar Pond, *International Journal of Thermal Science*, 47 (2008), 1, pp. 93-102
- [7] Karakilcik, M., *et al.*, Dynamic Exergetic Performance Assessment of an Integrated Solar Pond, *International Journal of Exergy*, 12 (2013), 1, pp. 70-86
- [8] Karakilcik, M., *et al.*, Performance Assessment of a Solar Pond with and without Shading Effect, *Energy Conversion and Management*, 65 (2013), Jan., pp. 98-107
- [9] Bozkurt, I., Karakilcik, M., The Daily Performance of a Solar Pond Integrated with Solar Collectors, *Solar Energy*, 86 (2012), 5, pp. 1611-1620
- [10] Bozkurt, I., *et al.*, An Investigation of the Effect of Transparent Covers on the Performance of a Cylindrical Solar Pond, *International Journal of Green Energy*, 11 (2014), 4, pp. 404-416
- [11] Bozkurt, I., *et al.*, Energy Efficiency Assessment of Integrated and Nonintegrated Solar Ponds, *International Journal of Low-Carbon Technologies*, 9 (2014), 1, pp. 45-51
- [12] Bozkurt, I., Karakilcik, M., The Effect of Sunny Area Ratios on the Thermal Performance of Solar Ponds, *Energy Conversion and Management*, 91 (2015), Feb., pp. 323-332
- [13] Bozkurt, I., Karakilcik, M., Exergy Analysis of a Solar Pond Integrated with Solar Collector, *Solar Energy*, 112 (2015), Feb., pp. 282-289
- [14] Bozkurt, I., *et al.*, Performance Assessment of a Magnesium Chloride Saturated Solar Pond, *Renewable Energy*, 78 (2015), June, pp. 35-41

- [15] Bozkurt, I., et al., A New Performance Model to Determine Energy Storage Efficiencies of a Solar Pond, *Heat Mass Transfer*, 51 (2015), 1, pp. 39-48
- [16] Bezir, N. C., et al., Numerical and Experimental Analysis of a Salt Gradient Solar Pond Performance with or without Reflective Covered Surface, *Applied Energy*, 85 (2008), 11, pp. 1102-1112
- [17] Nie, Z., et al., Experimental Study of Natural Brine Solar Ponds in Tibet, *Solar Energy*, 85 (2011), 7, pp. 1537-1542
- [18] Kayali, R., et al., A Rectangular Solar Pond Model Incorporating Empirical Functions for Air and Soil Temperatures, *Solar Energy*, 63 (1998), 6, pp. 345-353
- [19] Kumar, A., Kishore, V. V. N., Construction and Operational Experience of a 6000 m<sup>2</sup> Solar Pond at Kutch, India, *Solar Energy*, 65 (1999), 4, pp. 237-249
- [20] Saleh, A., et al., Performance Investigation of a Salt Gradient Solar Pond Coupled with Desalination Facility Near the Dead Sea, *Energy*, 36 (2011), 2, pp. 922-931
- [21] Bernad, F., et al., Salinity Gradient Solar Pond: Validation and Simulation Model, *Solar Energy*, 98 (2013), Part C, pp. 366-374
- [22] Akbarzadeh, A., et al., Examining Potential Benefits of Combining a Chimney with a Salinity Gradient Solar Pond for Production of Power in Salt Affected Areas', *Solar Energy*, 83 (2009), 8, pp. 1345-1359
- [23] Ranjan, K. R., et al., Energy and Exergy Analyses of Solar Ponds in the Indian Climatic Conditions, *International Journal of Exergy*, 15 (2014), 2, pp. 121-151
- [24] Bird, R. B., et al., *Transport Phenomena*, 2<sup>nd</sup> ed., John Wiley and Sons, New York, USA, 2007
- [25] Modest, M. F., *Radiative Heat Transfer*, 2<sup>nd</sup> ed., Academic Press, San Diego, Cal., USA, 2003
- [26] Fiveland, W. A., Selection of Discrete Ordinate Quadrature Sets for Anisotropic Scattering, *Fundamentals of Radiation Transfer*, Vol. 160, pp. 89-91, 1991
- [27] Duffie, J. A., Beckman, W. A., *Solar Engineering of Thermal Processes*, 4<sup>th</sup> ed., John Wiley and Sons, Inc. Published, New York, USA, 2013
- [28] Bryant, H. C., Colbeck, I., A Solar Pond for London, *Solar Energy*, 19 (1977), pp. 321-322